

Apparent Directional Emittances on the V-Groove and the Circular Groove Rough Surfaces*

by kimio KANAYAMA**

(Received march 31, 1971)

The radiations from the solid surfaces whose surface roughness is random are complicated phenomena. In this paper as a first step, therefore, are the apparent directional emittances of the simplified rough surfaces, supposing that these are composed of the same V-grooves and the same circular grooves, calculated two dimensionally, the emittances of the specimens of aluminum are measured experimentally, and the calculation values are compared with the measurement values.

1. Introduction

It is well known that the measured values of the directional emissivity on some metallic plane surfaces agree well with the values obtained by the approximate equation of the monochromatic emissivity developed by E. Schmidt and others^{(1),(2)} by way of the electromagnetic theory. But the characteristics of the directional emittances on the rough surfaces of metals will be different from those of the emissivity on the metallic plane surfaces, due to the statistic distribution of the dimensions and the shapes of the surface roughness. These are guessed from the details of the results from the experiments which are made by Birkebak⁽³⁾ of the directional reflectance on the rough surfaces of metals.

The complicated phenomena⁽⁴⁾, such as the interface and the diffraction of wave-motion, will be present on the region where the magnitude of radiation wave approaches the dimension of surface roughness.

In this report, therefore, in order to simplify the matter, a study was performed on the limited region where the dimension of roughness was far larger than the radiation wave-length.

The apparent directional emittances of the rough surfaces consisting of the V-grooves and the circular grooves of metals were analyzed by applying the results developed from the electromagnetic theory and were calculated numerically. The measurements of those on the surfaces of aluminum were carried out and the results of the theoretical analysis were proved by the experiments.

2. Theoretical Analysis

The apparent directional emittance is calculated on the following assumptions:

(1) The groove dimension is far larger than the wave-length of the radiation.

* Brief of the manuscript contributed to Bulletin of the JSME.

** Department of Mechanical Engineering, Kitami Institute of Technology.

(2) The inside surface of the groove is smooth, and its material has a specific property of the monochromatic directional emissivity of the metallic plane surface according to the results of the electromagnetic theory and has a specific property of the specular reflection.

An approximate equation⁵⁾ introduced by the electromagnetic theory is

$$\varepsilon_\varphi = \frac{1}{n} \left(\cos \varphi + \frac{1}{\cos \varphi} \right) \quad (1)$$

where n is the index of the refraction of materials, φ is an angle either of the emission, of the incidence, or of the reflection of the radiation beam and measured from the normal of the plane surface ($0^\circ \leq \varphi < 90^\circ$) and ε_φ is the directional emissivity in direction φ .

2.1 Apparent directional emittance of the V-groove opening

Fig. 1 shows the V-groove 101' which is made the object of analysis, and its image. Let us consider the radiation from the V-groove opening 1-1' in direction ϕ . It is the sum total of the emission component from P_1 on the inside surface and of the reflection components, one emitted from P'_2 on the opposite surface and reflected at P_1 ; the other, emitted from P'_3 on that surface, reflected at P_1 through P'_2 . Then the terms of the reflected components of the emission increase with the number of reflections.

The reflection beam in the V-groove is originally shown by a broken line $P_1P'_2P'_3$, but using the image technique⁶⁾ it is shown by a straight line $P_1P_2P_3$ crossing image lines. The number of times ($i-1$) that a straight line crosses the image lines indicates the maximum number of reflections, and also the angles either of the emission, of the incidence or of the reflection, can be obtained graphically.

The apparent directional emittance of radiation $\varepsilon_{\alpha\phi}$ which includes the components of reflections ($i-1$) and which emits in direction ϕ is

$$\varepsilon_{\alpha\phi} = \varepsilon_{\varphi_1} + (1 - \varepsilon_{\varphi_1}) \varepsilon_{\varphi_2} + (1 - \varepsilon_{\varphi_1})(1 - \varepsilon_{\varphi_2}) \varepsilon_{\varphi_3} + \dots + (1 - \varepsilon_{\varphi_1})(1 - \varepsilon_{\varphi_2})(1 - \varepsilon_{\varphi_3}) \dots (1 - \varepsilon_{\varphi_{i-1}}) \varepsilon_{\varphi_i} \quad (2)$$

where $i = 1, 2, 3, \dots$, and the first term = the emission component, the second term = the component of the reflection number one, the third term = the component of the reflection number two and so on, and the directional angle ϕ is measured from the normal on the groove opening, in a plane normal to groove axis.

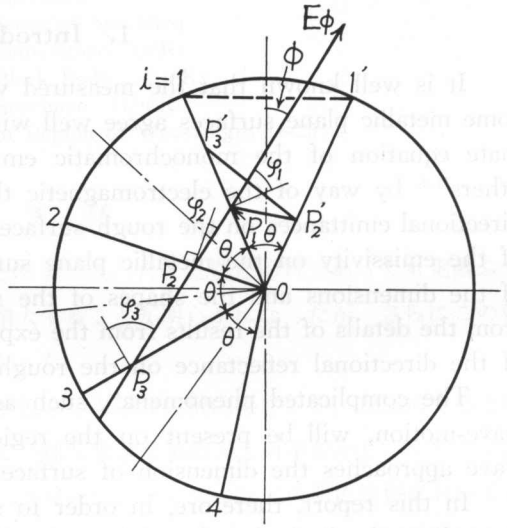


Fig. 1. Image technique on the analysis of emission from the V-groove.

Hence, we can get ε_{φ_i} substituting into Eq. (1) the angle φ_i of the emission, of the incidence or of the reflection, obtained graphically and further we can calculate the apparent directional emittance $\varepsilon_{\alpha\phi}$ substituting ε_{φ_i} into Eq. (2). The left part of Fig. 4 shows the calculated results in case the index of refraction $n=50$.

2.2 Apparent directional emittance of the opening of the circular groove

In Fig. 2, the mean wall emissivity ε_{φ_j} on an element of the concave whose emission consists of the components of reflections of the same number $(j-1)$ and which emits in direction φ_j measured from the normal at a point on the inside surface of the groove and in a plane normal to the groove axis is

$$\varepsilon_{\varphi_j} = \frac{\int_{\varphi_{j-1}}^{\varphi_j} \varepsilon_{\varphi} d\varphi}{\int_{\varphi_{j-1}}^{\varphi_j} d\varphi} \quad (3)$$

Integration of Eq. (3) from φ_{j-1} to φ_j after substituting Eq. (1) into Eq. (3), yields equation

$$\varepsilon_{\varphi_j} = \frac{\frac{1}{n} \cdot \int_{\varphi_{j-1}}^{\varphi_j} \left(\cos \varphi + \frac{1}{\cos \varphi} \right) d\varphi}{\int_{\varphi_{j-1}}^{\varphi_j} d\varphi} = \frac{\frac{1}{n} \cdot \left| \sin \varphi + \log_e \tan \left(\frac{\varphi}{2} + \frac{\pi}{4} \right) \right|_{\varphi_{j-1}}^{\varphi_j}}{\varphi_j - \varphi_{j-1}} \quad (4)$$

The sum total of the emittances $\sum \varepsilon_{\varphi_j}$, which consists of the components of reflections of the maximum number $(j-1)$, is represented by the next polynomial formula,

$$\sum \varepsilon_{\varphi_j} = \left\{ \varepsilon_{\varphi_j} + (1 - \varepsilon_{\varphi_j}) \varepsilon_{\varphi_j} + (1 - \varepsilon_{\varphi_j})^2 \varepsilon_{\varphi_j} + \dots + (1 - \varepsilon_{\varphi_j})^{j-1} \varepsilon_{\varphi_j} \right\} = 1 - (1 - \varepsilon_{\varphi_j})^j \quad (5)$$

where $j=1, 2, 3, \dots$

In the next place, the apparent directional emittance $\varepsilon_{\alpha\phi}$ on the groove opening is calculated from the sum of the results of multiplying $\sum \varepsilon_{\varphi_j}$ of each element by the weight $(l_j - l_{j-1})$ of its element, calculated assuming that the radius is unit one and on condition that the projected area is constant. That is

$$\varepsilon_{\alpha\phi} = \frac{1}{\cos \phi \cdot \cos \gamma} \sum_1^j \left\{ 1 - (1 - \varepsilon_{\varphi_j})^j \right\} \cdot (l_j - l_{j-1}) \quad (6)$$

where $(1/\cos \phi)$ is the compensation of the direction ϕ and $(1/\cos \gamma)$ is the compensation of the chord.

By substituting Eq. (4) into Eq. (6), the equation (7) yields.

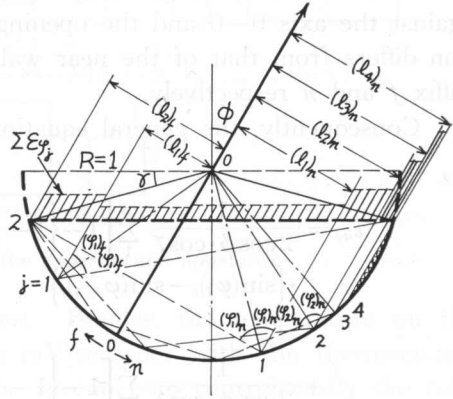


Fig. 2. Analytical method of emission from the circular groove.

$$\varepsilon_{a\phi} = \frac{1}{\cos\phi \cdot \cos\gamma} \sum_1^j \left[1 - \left\{ 1 - \frac{1}{n} \cdot \frac{\left| \sin\varphi + \log_e \tan\left(\frac{\varphi}{2} + \frac{\pi}{4}\right) \right|_{(\varphi_{j-1})}^{\varphi_j}}{\varphi_j - \varphi_{j-1}} \right\}^j \right] \cdot (\sin\varphi_j - \sin\varphi_{j-1}). \quad (7)$$

Where, since ϕ is generally unequal to zero, the opening is asymmetrical against the axis 0-0 and the opening of the far wall from the emitting direction differs from that of the near wall, so these are distinguished by the use of suffix f and n respectively.

Consequently, the general equation of $\varepsilon_{a\phi}$ is written in the form

$$\begin{aligned} \varepsilon_{a\phi} = & \frac{1}{2\cos\phi \cdot \cos\gamma} \sum_1^j \left[1 - \left\{ 1 - \frac{1}{n} \cdot \frac{\left| \sin\varphi + \log_e \tan\left(\frac{\varphi}{2} + \frac{\pi}{4}\right) \right|_{(\varphi_{j-1})_f}^{(\varphi_j)_f}}{(\varphi_j)_f - (\varphi_{j-1})_f} \right\}^j \right] \\ & \cdot \left\{ \sin(\varphi_j)_f - \sin(\varphi_{j-1})_f \right\} \\ & + \frac{1}{2\cos\phi \cdot \cos\gamma} \sum_1^j \left[1 - \left\{ 1 - \frac{1}{n} \cdot \frac{\left| \sin\varphi + \log_e \tan\left(\frac{\varphi}{2} + \frac{\pi}{4}\right) \right|_{(\varphi_{j-1})_n}^{(\varphi_j)_n}}{(\varphi_j)_n - (\varphi_{j-1})_n} \right\}^j \right] \\ & \cdot \left\{ \sin(\varphi_j)_n - \sin(\varphi_{j-1})_n \right\} \end{aligned} \quad (8)$$

$$\text{where } \begin{cases} (\varphi_j)_f = \frac{\pi}{2} \cdot \frac{2j - \left(1 + \frac{2\phi}{\pi}\right) + \frac{2\gamma}{\pi}}{2j+1} \\ (\varphi_j)_n = \frac{\pi}{2} \cdot \frac{2j - \left(1 - \frac{2\phi}{\pi}\right) + \frac{2\gamma}{\pi}}{2j+1} \\ \text{at } j=0, \quad (\varphi_0)_f = (\varphi_0)_n = 0. \end{cases}$$

The apparent directional emittances are computed from Eq. (8) in each case they contain no component of the reflection; $j=1$, the components of two reflections at maximum; $j \leq 3$, or the components of the nineteen reflections at maximum; $j \leq 20$. The calculated results are shown in the left part of Fig. 5, where it is computed on $n=50$, $j \leq 3$.

3. Experimental Procedure

Fig. 3 shows the schematic diagram of the main parts of experimental apparatus. The outline of the experimental procedure is as follows:

In Fig. 3, a specimen is fixed on the heater and is heated at a constant temperature ($200 \pm 2^\circ\text{C}$). The radiation beam emitted from the surface of the specimen reaches the concave mirror through the aperture of the shield ($10 \text{ mm} \times 10 \text{ mm}$) and the slit ($10 \text{ mm} \times 4 \text{ mm}$) and is collected in the focus. A vacuum thermocouple detector (Japan Spectroscopic Co.) is set in the focus. The output detected on the radiometer is measured with a DC-amplifier (Ohokura Electric Co. AM-1001). The temperature of the specimen is obtained by measuring with a mV-meter the output from the thermocouple (chromel-alumel wire 0.32ϕ)

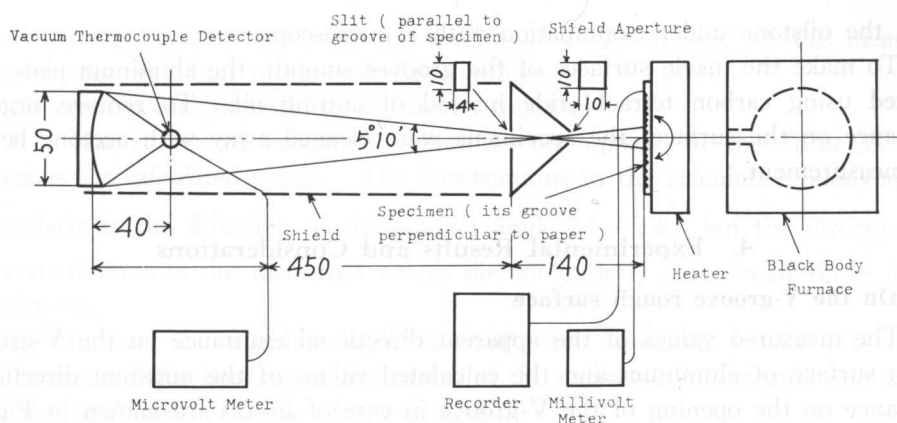


Fig. 3. Schematic diagram of the experimental apparatus.

which is set in the center of the specimen. Besides, the temperature on the periphery of the specimen is recorded in a mV-recorder with the thermocouple of the same type set in the periphery of the specimen to control easily the voltage of the source of the heater with a slidac and to check the temperature distribution of the specimen. So the temperature difference on the center and the periphery of the specimen was less than 1%.

As the assembly consisting of the specimen and the heater can be rotated about the vertical axis lying in the plane of the specimen surface and perpendicular to the plane of the figure, so the directional emittance can be measured in any direction. The radiometer response had been calibrated with a black body furnace maintained at the same distance as the optical path and the same temperature as in measuring the radiation from the sample.

Consequently, the absolute value of radiation energy can be detected and the emittance of specimen can be obtained by the ratio of both energies from the aperture of the black body furnace and from the surface of heated specimen.

Because the detector indication is measured, for convenience, without the radiation incidence being chopped, it is affected delicately by the room temperature, and because KBr (pass on $0\sim 25\ \mu$), or KRS-5 (pass on $0.7\sim 50\ \mu$), whose properties are deliquescent, are used for the hole materials of the detector, the laboratory is controlled at a constant temperature of $20\sim 21^\circ\text{C}$ and in humidity below 45% using an air conditioner.

The aluminum plates (JIS 1st class) with dimension of 115 mm by 115 mm and 5 mm thick were used for the specimens and the flawless rolled surfaces of those plates were used for the smooth surfaces of the specimens.

The V-groove and the circular groove rough surfaces are prepared by machining the aluminum plate with the shaper at various pitches, the tips of whose tools are shaped V or circular.

The V-shaped tools with a constant nose angle were prepared with a cutter grinder, and the circular shaped tool was prepared with a tip end which, after being ground off to 2 mm in width, was made semicircular in shape by whetting

it on the oilstone under examination with a microscope.

To make the inside surfaces of the grooves smooth, the aluminum plate was worked using carbon tetrachloride instead of cutting oil. To remove organic substance on the surface, the specimens were cleaned away with acetone before the measurement.

4. Experimental Results and Considerations

4.1 On the V-groove rough surface

The measured values of the apparent directional emittance on the V-groove rough surface of aluminum and the calculated values of the apparent directional emittance on the opening of the V-groove in case of $n=50$ are shown in Fig. 4.

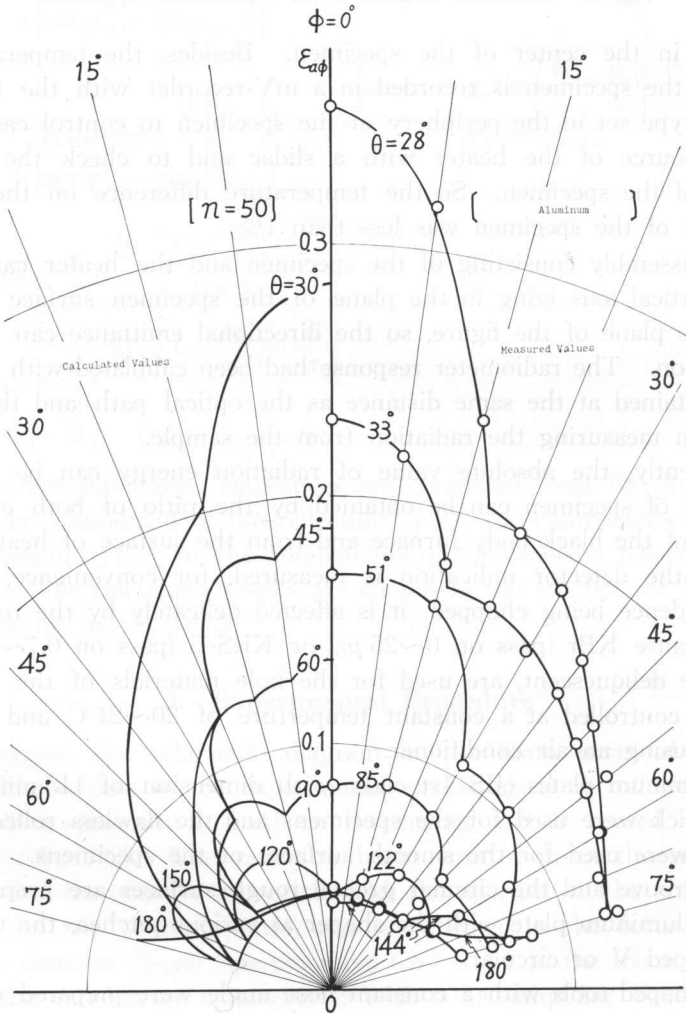


Fig. 4. Calculated values (left hand) and measured values (right hand) of apparent directional emittance of the V-groove rough surfaces.

By comparing both, as a whole, the tendency of the change of the measured values agrees well that of the calculated values.

Different points in both values are as follows :

(1) The curves of measured values do not appear to be from as clear shapes as the calculated values. The constrictions in the calculated values appear particularly in the direction of the contact angle $\left(\phi = \frac{1}{2}\theta\right)$, but the directions of the constrictions in the measured values do not entirely agree with those in the calculations.

(2) In case the opening angle is small, the measured values exceed the calculations and the bottoms of the curves of the measurements expand as a whole, with the increment of angle of the direction.

(3) The measured value of the vertical emittance on the rough surface of the opening angle $\theta = 144^\circ$ is smaller than the calculated value in each case of $\theta = 150^\circ$ and $\theta = 180^\circ$ (plane).

The reasons for these are considered as follows :

The reason for (1) will be due to the incompleteness in shape of the V-groove, the insufficient smoothness of the inside surfaces of the groove and the solid angle ($5^\circ 10'$) when the radiation passes through the slit.

The reason for (2) will be that, in case the opening angle is small, the top of the groove is roughened and the rate it occupies in the field through the slit increases in proportion to the increment of the directional angle, so that its apparent emittance increased.

The reason for (3) will be that, even if the smooth surface has the maximum roughness $H_{\max} = 0.4 \mu$, while as the shallow groove of the large opening angle is created in the very smooth inside surface, the decrease of the emittance due to the rise in smoothness exceeds the increase of the emittance due to the angle factor itself, so that it becomes small close to the value of the wall emissivity of aluminum.

The index n of pure aluminum is nearly 69 at 200°C , according to the results of the calculation applying the electromagnetic theory. The measured values, however, agreed well with the calculated values at $n=50$ rather than at $n=70$. This difference will be occasioned by the existence of impurities in the interior and on the surface of aluminum, and the microroughness of the inside of the groove.

4.2 On the circular groove rough surface

The measured values of the apparent directional emittance on the circular groove rough surface of aluminum and the calculated values of the apparent directional emittance on the opening of the circular groove, in case of $n=50$, $j \leq 3$, are shown in Fig. 5.

By comparing both, the tendency of the change of measured values is found to agree well with that of the calculated values as a whole.

What are different in both values are the following three points :

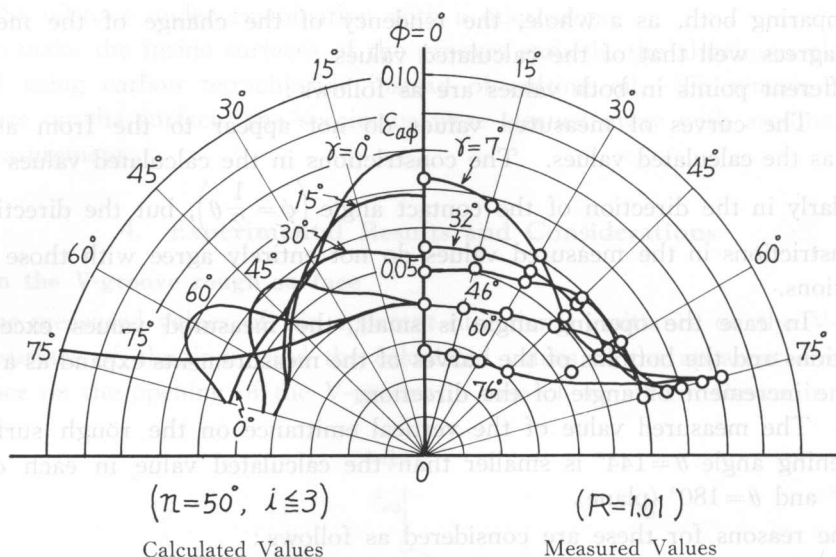


Fig. 5. Calculated values and measured values of apparent directional emittance of the circular groove rough surfaces.

(1) The swellings of the curves of the calculated values appear clearly in direction $\phi = \gamma$, but those of the measured values are not so clear.

(2) In case the deflection angle from semi-circular γ is small, in proportion to the increment of the angle ϕ , the measured values exceed the calculations and the bottoms of curves of the measurements show a tendency to expand as a whole.

(3) Together with the increment of γ , the measured values are smaller than the calculations.

The reasons for these are considered as follows:

The reason for (1) will be due to the incompleteness of the groove incircularity and the diffused reflections due to the microroughness of the inside surface of the groove. For these reasons, a great number of reflections on the inside surface are not expected, so that it seems that the measured values approximate to the calculations in case of $j \leq 3$.

The reason for (2) will be that when the groove becomes deep by decreasing γ , the emittance increases due to the increment of the roughness of the upper sides of the groove and its influence comes about when the directional angle ϕ is large.

The reasons for (3) and for the fact that the measured values approximate to the calculations in $n=50$, $j \leq 3$ as a whole, will be the same as in the case of the V-groove.

Theoretical calculations are made of the monochromatic emittance and experimental measurements are taken of the total emittance, but fine agreements are obtained between both values. The reason is that according to the results which the authors⁷⁾ obtained in carrying out the measurement of the spectral emittances of the smooth and rough surfaces of aluminum, the spectral emittances

of these aluminum surfaces are nearly constant against the wavelength of radiation, and it seems that also the properties of the grooved rough surfaces of aluminum are approximately the so-called gray body.

5. Conclusions

The apparent directional emittances of the V-groove and the circular groove rough surfaces were calculated by application of the property of the directional emissivities, introduced by the electromagnetic theory, to the inside surfaces of the grooves and summing up the emission components and the reflection components on the surface elements of the grooves.

At the same time, the apparent directional emittances of the specimens of the V-groove or the circular groove of aluminum were measured at 200°C, and the measured values agreed well with the calculated values as a whole.

Acknowledgment

The author expresses his heartfelt thanks to Dr. Takeshi Saito, Professor of Mechanical Engineering, Faculty of Technology, University of Hokkaido, for his suggestion of this study object.

References

- 1) E. Schmidt and E. Eckert: *Forschung Gebiete Ing.*, **6**, 175 (1935).
- 2) M. Jakob: *Heat Transfer*, **1**, 44 (1964), Wiley.
- 3) R. C. Birkebak and E. R. G. Eckert: *Trans. ASME., J. Heat Trans.*, **87**, Ser. C, 1, 85 (1965).
- 4) H. Hasunuma: *Luster*, 68 (1965), Tokyo.
- 5) same as 1), 47.
- 6) R. B. Zipin: *J. Resh. Nat. Bur. Stand.*, 70 C-4, 275 (1966).
- 7) K. Kanayama and H. Baba: Paper of 7th Heat Transfer Symposium of Japan, 301 (1970).